32nd EPS Conference on Plasma Phys. Tarragona, 27 June - 1 July 2005 ECA Vol.**29C**, O-3.006 (2005)

Experiment vs. Theory on Electric Inhibition of Fast Electron Penetration of Targets

R.R. Freeman[1,2], K. Akli[2], D. Batani[3], S. Baton[4], S. Hatchett[5], D. Hey[2], M. Key[5], J. King[2]
A. MacKinnon[5], P. Norreys[6], R. Snavely[5], R. Stephens[7], C. Stoeckl[8], R. Town[5], B. Zhang[2]

[1] *The Ohio State University, Columbus, OH, USA*

[2] *University of California-Davis, Davis, CA, USA*

[3] *Departimento di Fisica "G. Occhialini", Universita' di Milano Bicocca, Milano, Italy*

[4] *LULI, Ecole Polytechnique, Palaiseau, France*

[5] *The University of California, LLNL, Livermore, CA, USA*

[6] *Rutherford Appleton Laboratories, Didcot, Oxfordshire, UK*

[7] *General Atomics, San Diego, CA, USA*

[8] *Laboratory for Laser Energetics, Rochester, NY, USA*

In this paper we present experimental results of penetration images of fast electrons in normal density materials using a high resolution crystal imaging system transverse to the electron flow. Our results show striking images that provide obvious evidence of the electric inhibition, as well as the lateral spreading of the fast electrons.

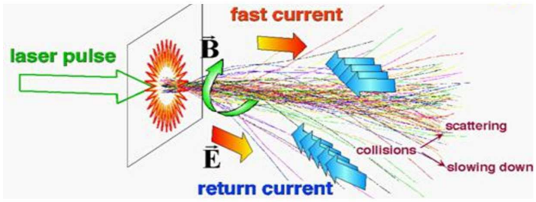

Hybrid PIC model (Paris) C. Toupin et al. In Inertial Fusion Science and Applications 99 Publ. Elsevier p471 (2000)

Figure 1: Fast electron transport within solid material is complicated by the generation of electric and magnetic fields

A dominant force of inhibition of fast electrons in normal density matter is due to an axially directed electrostatic field (Fig. 1). Fast electrons leave the critical density layer and enter the solid in an assumed relativistic Maxwellian energy distribution. The charge separation is neutralized by a background return current density $j_b = en_b\upsilon_b$ equal and opposite to the fast electron current density $j_f = en_f\upsilon_f$ [1] where it is assumed that the fast electron number density is much less than the background number density, $n_f \ll n_b$ [2]. This charge and current neutralization allows the forward moving fast electron current to temporarily exceed the Alfven limit by many orders of magnitude [3]. During this period the cold return current, in passing through the material resistivity, η, ohmically generates an electric field $E = j_c\eta$ in opposition to the fast current. As a result, the fast electron current loses its energy to the material, via the return current, in the form of heat [4].

The material resistivity, η, is a function of the material temperature and so as the current channel is ohmically heated by the slow counter-propagating electrons, η changes. In general, the variation of resistivity with temperature and density can be divided into two regimes of temperature [5]. As shown in figure 2, at low temperatures the resistivity rises rapidly with temperature and plateaus at 2 μ Ω m in the range of 10 to 100 eV for most all materials. Notice also that in this "cold" regime the resistivity has a strong inverse dependence on the density. At temperatures beyond the plateau, the $T^{-3/2}$ dependence of the Coulomb cross section for electron-ion scattering begins to dominate and the resistivity diminishes with temperature. In this so called "Spitzer" regime, the resistance is a very weak function of density through the coulomb logarithm.

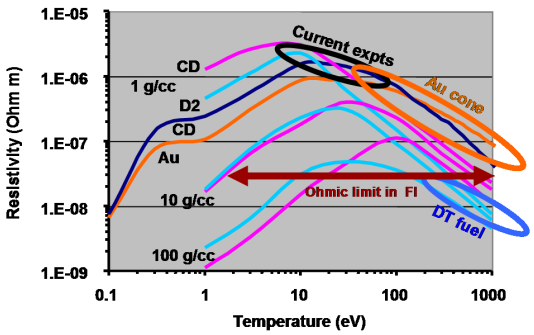

Figure 2: Resistivity vs. temperature

Electron transport experiments were conducted at the Vulcan laser within the Rutherford Appleton Laboratory in the UK. An 81J, 800fs 1053 nm Nd:glass laser pulse was focused to 10 μm by an f/3 off-axis parabolic mirror onto the thin edge of a solid 50%/50% (by mass) amalgam of Cu and Al as shown in figure 3. The laser spot was positioned $\sim$50 μm from the edge on the observation side. A 1.6 cm apertured SiO2 $21\bar{3}1$ quartz crystal, bent to a radius of 38 cm and operating at 1.3^0 off normal incidence, transversely viewed Cu Kα x-rays from the Cu/Al amalgam and produced a 7.9x magnified image onto a Princeton Instruments, 1 square inch, 1024×1024 pixel CCD internally cooled to -30 C. Astigmatism and spherical aberration limited spatial resolution to 10 μm.

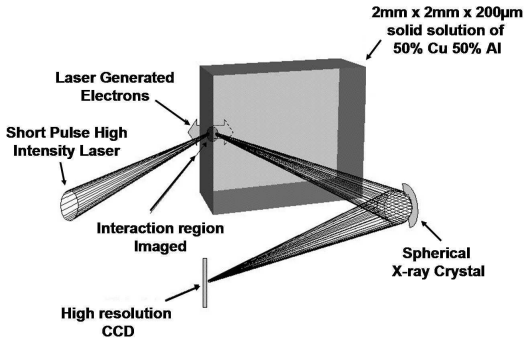

Figure 3: A spherically bent crystal was used to image Cu Kα X-rays from the Cu/Al amalgam onto a CCD.

A typical image from these experiments is shown in figure 4. The laser was normally incident to the thin edge of the target and rotated 53^0 from the viewing axis. The image shows very shallow fast electron spreading into a 90 μm spot and strongly attenuated penetration into the solid.

Corrections applied to account for the oblique viewing angle and an assumed 40^0 deep spreading of the fast electrons [6] determined the $1/e$ attenuation length to be about 100 μm. These results are consistent with findings in the rear-view buried-layer Kα studies of Stephens *et al* [6].

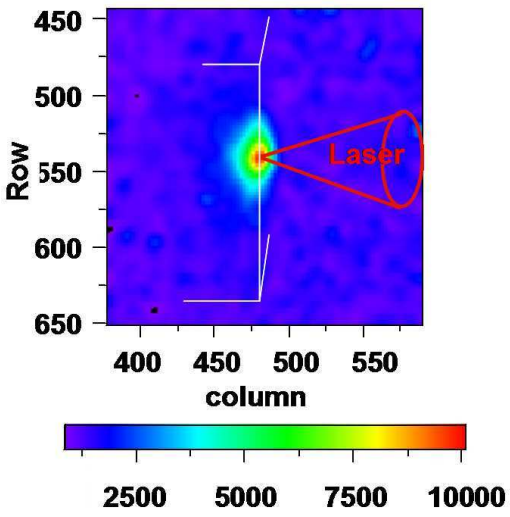

Figure 4: CCD image of Cu Kα from a solid Cu/Al amalgam. At 53^0 from the laser axis, the image provides a semi-transverse view of the electron flux within the solid.

An image of a shot similar to the previous except with a 500 μm long gold cone attached is shown in figure 5. The $\leq$30 μm diameter cone tip was attached with the cone axis normal to the thin edge at a distance of 50 μm from the observation side. Comparison of the two images in figures 4 and 5 indicates similar front surface spreading and fast electron penetration. It is also seen that the signal level of the cone shot is nearly an order of magnitude lower than that of the no-cone shot. This is most likely due to attenuation of the hot electron current through 5 μm of Au at the cone tip.

With laser intensities of 1.9×10^{20} W/cm^2 and resulting average electron energies of 1.5 MeV, collisional stopping alone predicts a maximum electron range of $\sim$1mm and thus cannot account for the observed attenuation lengths of $\sim$100 μm. A simple model of electric inhibition in which the average fast electron energy is equated to an ohmic stopping potential yields an electron range of $\sim$395 μm. Combining these effects gives a maximum stopping range of $\sim$280 μm which agrees more closely with observations. As indicated in figure 2, the normal densities and low temperatures of the materials shot in this experiment and, in fact, all of our FI-related experiments on electron transport to date [7], maximize the resistivity and thus maximize the electric inhibition. In contrast, full scale fast ignition transport will occur within high density (300 g/cm^3),

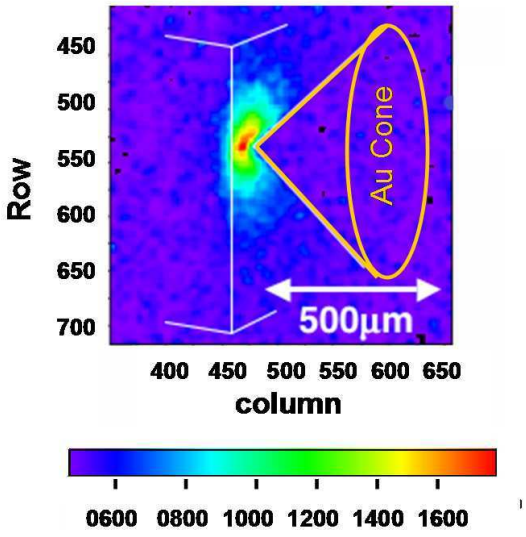

Figure 5: A Au cone has been attached to guide the laser pulse. Electron surface spreading and transport inhibition differs little from the no-cone image.

high temperature ($\sim$ 1 keV) cores [9] which have resistivities lower by two orders of magnitude.

It has been suggested that the very large initial source size consistently observed in our experiments could be attributed to an extended spatial profile of the beam. If the 90 μm diameter spot size observed in the no-cone shot were due to the laser intensity profile, then adding a cone which tapers to a 30 μm diameter tip would clip this intensity resulting in a much smaller source diameter. However, as seen by comparison of figures 4 and 5, there is no significant reduction in source size with the use of a cone and therefore it appears that the large source size is not due to the laser intensity profile.

One possible physical mechanism for source spreading is a radially directed force due to crossed **E** and **B** fields within the pre-plasma [8]. An axial **E** field results from pre-pulse "blow off" and an azimuthal **B** field results from $\nabla \mathbf{N} \times \nabla \mathbf{T}$ within the pre-plasma. The radial drift velocity is proportional to $(\mathbf{E}\times\mathbf{B})/\mathbf{B}^2$. To spread electrons 30$\mu$m radially in the $\sim$1ps time scale of the experiments requires a velocity > 3×10^9 cm/s [6]. This could be obtained, for example, with a 1 MG **B** field and a 3keV/μm **E** field, both reasonable values for these experiments.

In conclusion, penetration depth and surface spreading as determined from transverse Cu Kα imaging of Cu/Al amalgam targets are in good agreement with rear-surface Kα imaging studies. In our experiments, electron transport has been dominated by electric inhibition and until higher temperature, higher density experiments are accessible, it may be feasible for transport studies to go to higher density shocked materials in which the resistivity is decreased and higher penetration is possible. The possibility of surface spreading due to the non-negligible intensity within the wings extended laser intensity profiles has been eliminated. Spreading is now thought to be partly due to crossed **E** and **B** fields which develop within the pre-plasma.

References

[1] A. Bell, J. Davies, S. Guerin, and H. Ruhl, Plasma Phys. Control Fusion **39**, 653 (1997)

[2] D. Hammer and N. Rostoker, Phys. Fluids **13**, 1831 (1970)

[3] J. Davies, Phys. Rev. E **68**, 056404 (2003)

[4] J. Davies, A. Bell and M. Haines Phys. Rev. E **56**, 7193 (1997)

[5] H. Milchberg, R. Freeman and S. Davey Phys. Rev. Lett. **61**, 2364 (1988)

[6] R. Stephens et al, Phys. Rev. E **69**, 066414 (2004)

[7] R. Freeman, et al (to be published)

[8] D. Forslund and J. Brackbill, Phys. Rev. Lett. **61**, 2364 (1988)

[9] M. Tabak et al, Phys. Plasmas **1**, 1626 (1994)